Supplementary Information (SI) for Green Chemistry.
This journal is © The Royal Society of Chemistry 2025

Supplementary Materials for

Metal-carbon electrode optimization for efficient electrochemical regeneration of 1,4-NADH: a new approach for sustainable biochemical synthesis

Yang Zhou[ab], LingLong Huang[ab], Yuan Tao[ab], ChangQing Luo[ab], JianMiao Xu*[ab], ZhiQiang Liu[ab], YuGuo Zheng[ab]

[a]*The National and Local Joint Engineering Research Center for Biomanufacturing of Chiral Chemicals, Zhejiang University of Technology, Hangzhou 310014, China.*

[b]*Key Laboratory of Bioorganic Synthesis of Zhejiang Province, College of Biotechnology and Bioengineering, Zhejiang University of Technology, Hangzhou 310014, China.*

***Corresponding author:**

Jian-Miao Xu, Key Laboratory of Bioorganic Synthesis of Zhejiang Province, College of Biotechnology and Bioengineering, Zhejiang University of Technology, Hangzhou 310014, China

E-mail: xujianmiao@zjut.edu.cn

Preparation of metal-carbon electrodes

Carbon nanopowder, activator (KOH), ethanol, and water were mixed in a round-bottom flask using magnetic stirring for 24 hours to form a composite. The mixture was subsequently dried in an oven at 80°C and then calcined in a muffle furnace at 800°C for 8 hours, followed by natural cooling to room temperature. The resulting material was rinsed with water, and the pH was adjusted to 7.0 by adding 30 mmol/L HCl, after which it was dried. Next, a composite of carbon, metal, and binder was prepared in a ratio of 8:1:1. This mixture was thoroughly blended for 4 hours to obtain a homogeneous and thin coating on the surface of the titanium foam and nickel-molybdenum foam electrodes, with a coating thickness of approximately 0.2 mm. The electrodes were then dried in a vacuum oven at 80°C and sintered in a muffle furnace at 200°C. The final product is a metal-carbon electrode.

Pretreatment of electrode materials

Metal sheet electrodes, 3D porous metal electrodes, and metal-carbon electrodes were subjected to a purification process to remove insoluble impurities. Initially, the electrodes were submerged in anhydrous ethanol for 24 hours. Subsequently, they were meticulously extracted and thoroughly cleansed with deionized water. To ensure the complete elimination of any residual impurities from the electrode surfaces, ultrasonic cleaning was employed. Ultimately, the electrodes were positioned in an oven to facilitate the complete evaporation of any remaining water and ethanol.

Configuration of the reaction system

Electrochemical experiments were conducted to investigate the electrochemical reduction of the oxidized form of nicotinamide adenine dinucleotide (NAD^+) to 1,4-NADH. The experimental setup comprised a constant potentiostat (Cinnabar Electrochemistry Workstation, model CHI600C), a thermostatic water bath stirrer, and a homemade three-electrode electrochemical cell. To prepare the NAD^+ solution, a 100 mL volume of a 5 mmol/L solution was formulated using phosphate buffer solution (PBS) at pH 7.4. The working electrode was a pre-treated metal electrode with a geometric surface area of 9 cm^2. Graphite and a $Pt|Hg(I)Hg_2Cl_2(s)|KCl$ electrode were employed as the auxiliary and reference electrodes, respectively. The entire reaction system was maintained at 308 K on a thermostatic water-bath stirrer, as this temperature is deemed optimal for enzymatic activity in most biocatalytic processes. The experimental setup is detailed in Supplementary Material S1.

Electrochemical regeneration of 1,4-NADH using metal-carbon electrodes

We conducted an investigation into the electrochemical regeneration of 1,4-NADH utilizing a 0.1 mol/L phosphate buffer solution and a 5 mmol/L NAD^+ solution. Various working electrodes were employed, comprising titanium foam, nickel-molybdenum foam, nickel-molybdenum-carbon, and titanium-carbon electrodes. The design of the electrochemical experiments was predicated on the outcomes derived from cyclic voltammetry. For the titanium-foam and titanium-foam-carbon electrodes, the applied potentials spanned from -0.5V to -1.1V. For the nickel-molybdenum-foam and nickel-molybdenum-foam-carbon electrodes, the potentials were configured within a range from -1.1 V to -1.7 V. The optimal reaction conditions for the reduction of 1,4-NADH were determined by integrating the current-time method with a reaction temperature of 308 K and a rotation speed of 300 rpm.

Detection methods

Cyclic voltammetry was conducted to acquire cyclic voltammograms for 5 mmol/L NAD^+ electrolyte solutions. Graphite and a $Pt|Hg(l)Hg_2Cl_2(s)|KCl$ electrode were employed as the auxiliary and reference electrodes, respectively. The voltage range was predetermined based on the specific electrode material, with a scanning rate set at 10 mV/s and a sampling interval of 1 mV. To comprehensively characterize and analyze the system, a suite of techniques was utilized, encompassing field emission scanning electron microscopy (SEM), energy-dispersive X-ray spectroscopy (EDS), X-ray photoelectron spectroscopy (XPS), X-ray diffraction (XRD), and Raman spectroscopy. These methodologies provided valuable insights into the mechanisms of coenzyme conversion on electrode surfaces. The yield of regenerated 1,4-NADH was determined by 1,4-NADH determination and quantification using a Biotronik NAD+ /NADH assay kit (WST-8 method) and UV-visible spectrophotometer. Furthermore, the yield of L-2-aminobutyric acid was assessed by high-performance liquid chromatography (HPLC) employing a C-18 column with a detection wavelength of 360 nm. The mobile phase was prepared by dissolving 5.012 g of sodium dihydrogen phosphate dodecahydrate in 700 mL of water and 300 mL of acetonitrile. The column temperature was maintained at 30°C, and the flow rate was set at 1 mL/min.

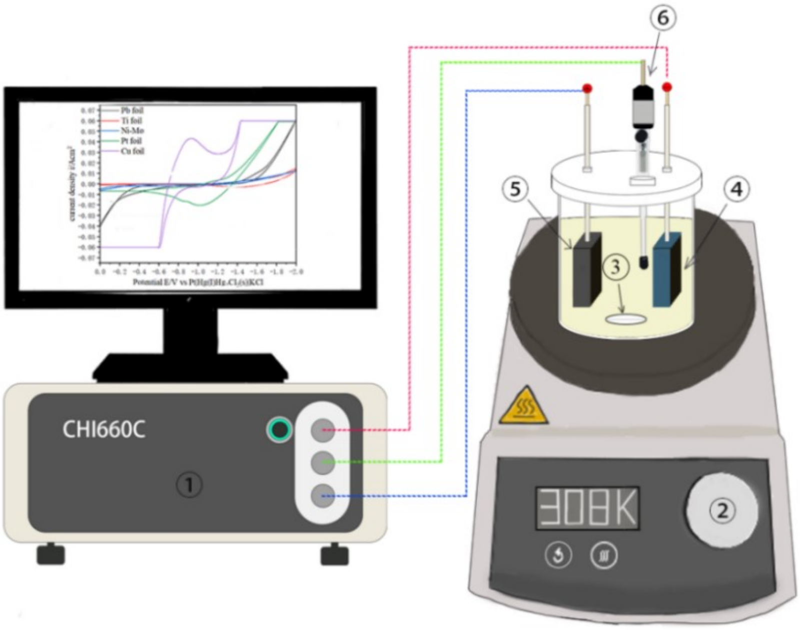

Figure S1. Schematic diagram of the electrochemical regeneration reactor setup for 1,4-NADH. Reactor setup components: (i) potentiostat; (ii) thermostatic stirrer (temperature and agitation); (iii) rotor; (iv) working electrode; (v) auxiliary electrode; (vi) reference electrode.

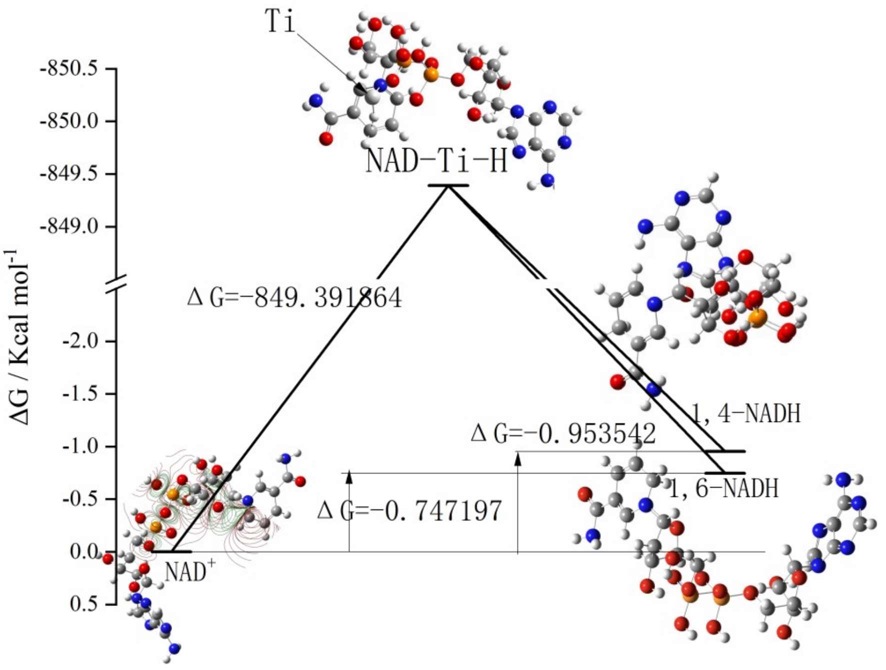

Figure S2. Principle and Analysis of NAD^+ Electrochemical Reduction to NADH, Focusing on Metal Foil Electrodes. The Gibbs Free Energy for the conversion of NAD^+ to various products was calculated using titanium (Ti) as the working electrode through computer modeling.

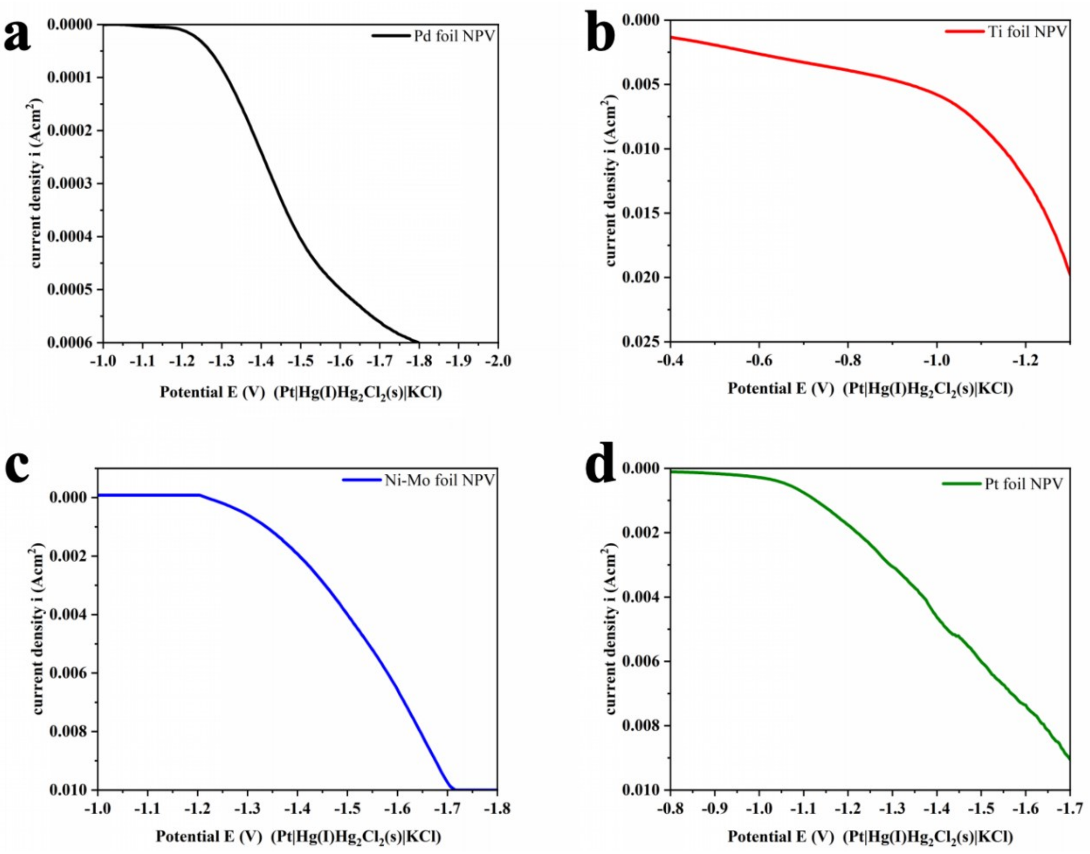

Figure S3. Normal pulse voltammograms of four conventional sheet metal electrodes. (a) Normal pulse voltammogram of metal Pd electrode regenerating coenzyme 1,4-NADH, scan rate 100 mV/s; (b) Normal pulse voltammogram of metal Ti electrode regenerating coenzyme 1,4-NADH, scan rate 100 mV/s; (c) Normal pulse voltammogram of metal Ni-Mo alloy electrode regenerating coenzyme 1,4-NADH, scan rate 100 mV/s; (d) Normal pulse voltammogram of metal Pt electrode regenerating coenzyme 1,4-NADH, scan rate 100 mV/s.

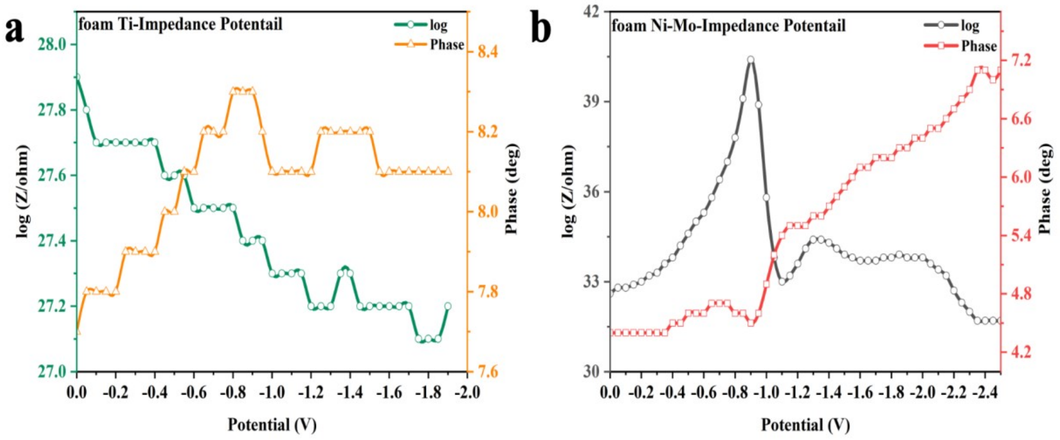

Figure S4. AC impedance-potential relationships for two foam metal electrodes. (a) Foamed titanium electrode AC impedance-potential relationship plot; (b) Foamed nickel-molybdenum alloy electrode AC impedance-potential relationship plot

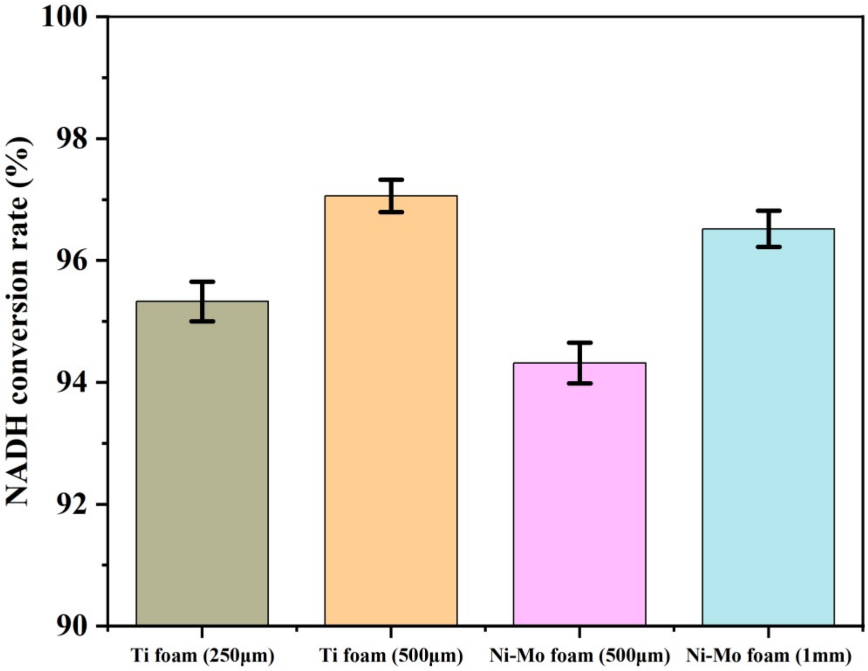

Figure S5. Effect of foam electrodes with different pore sizes on coenzyme 1,4-NADH. 1,4-NADH conversion of titanium foam electrodes with pore sizes of 250 μm and 500 μm and 1,4-NADH conversion of nickel-molybdenum alloy foam electrodes with pore sizes of 500 μm and 1 mm.

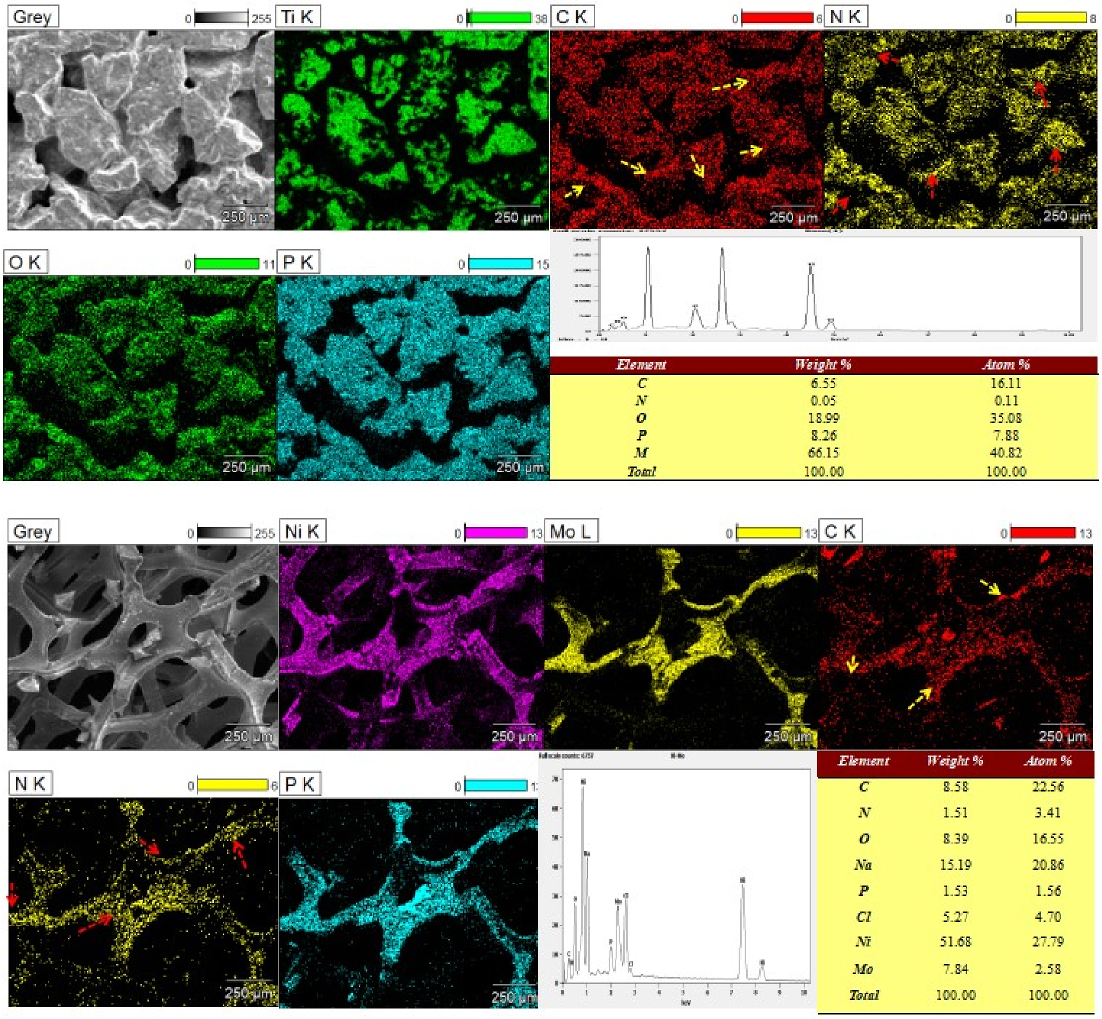

Element	Weight %	Atom %
C	6.55	16.11
N	0.05	0.11
O	18.99	35.08
P	8.26	7.88
M	66.15	40.82
Total	100.00	100.00

Element	Weight %	Atom %
C	8.58	22.56
N	1.51	3.41
O	8.39	16.55
Na	15.19	20.86
P	1.53	1.56
Cl	5.27	4.70
Ni	51.68	27.79
Mo	7.84	2.58
Total	100.00	100.00

Figure S6. Foam metal-bonded discrete carbon nanoelectrode field emission scanning electron microscopy (SEM) coupled with X-ray spectroscopy (EDS) diagrams. (A) Foam titanium-bonded discrete carbon nanoelectrode surface electron microscopy diagrams, as well as elemental distributions and elemental contents of titanium and carbon on the electrode surface. (B) Surface electron micrographs of the foam Ni-Mo bonded discrete carbon nanoelectrode and the elemental distribution and content of nickel, molybdenum and carbon on the electrode surface.

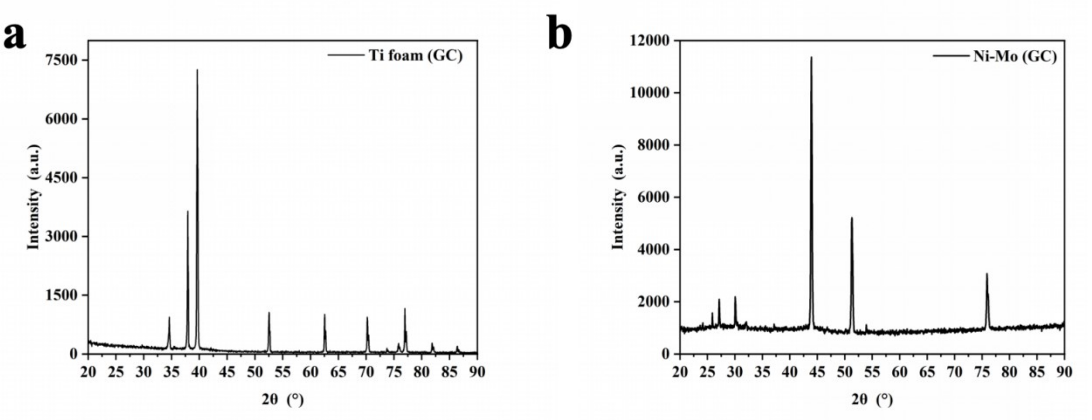

Figure S7. X-ray diffraction (XRD) of foam metal-bound discrete carbon nanoelectrode. (A) X-ray diffraction (XRD) pattern of the surface of foam titanium-bound discrete carbon nanoelectrode. (B) X-ray diffraction (XRD) pattern of the surface of foam Ni-Mo bonded discrete carbon nanoelectrode.

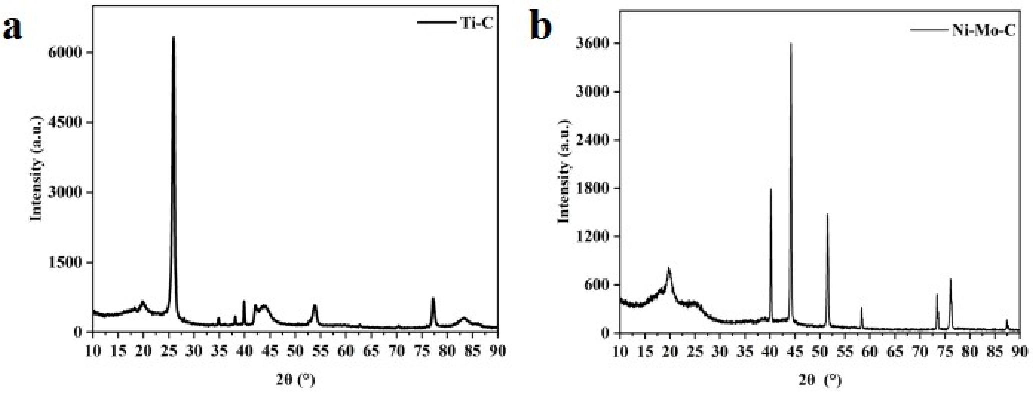

Figure S8. X-ray diffraction (XRD) of a homemade foam metal-carbon electrode. (A) X-ray diffraction (XRD) pattern of the surface of a foam titanium-carbon electrode. (B) Surface X-ray diffraction (XRD) pattern of foam Ni-Mo-C electrode.

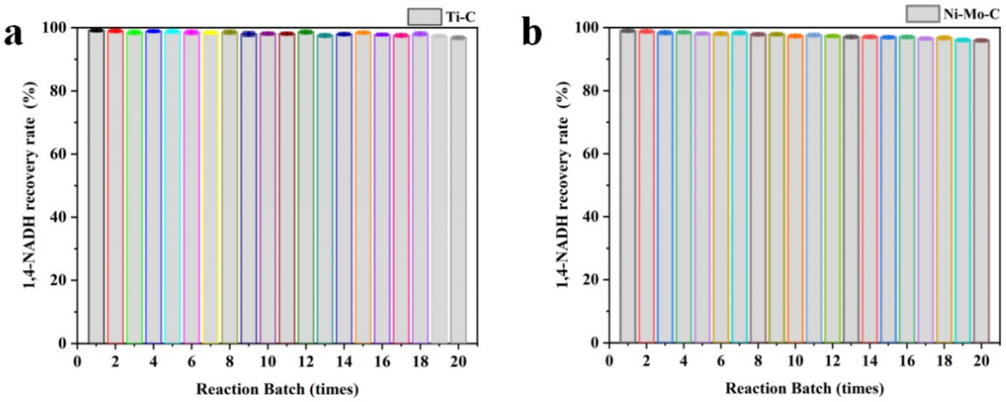

Figure S9. 20 replicate experiments using two homemade electrodes. (a) 20 electrochemical 1,4-NADH regeneration experiments using a homemade Ti-C composite electrode on a concentration of 5 mmol/L NAD$^+$ reaction solution (b) 20 electrochemical 1,4-NADH regeneration experiments using a homemade Ni-Mo-C composite electrode on a concentration of 5 mmol/L NAD$^+$ reaction solution for 20 electrochemical 1,4-NADH regeneration experiments.

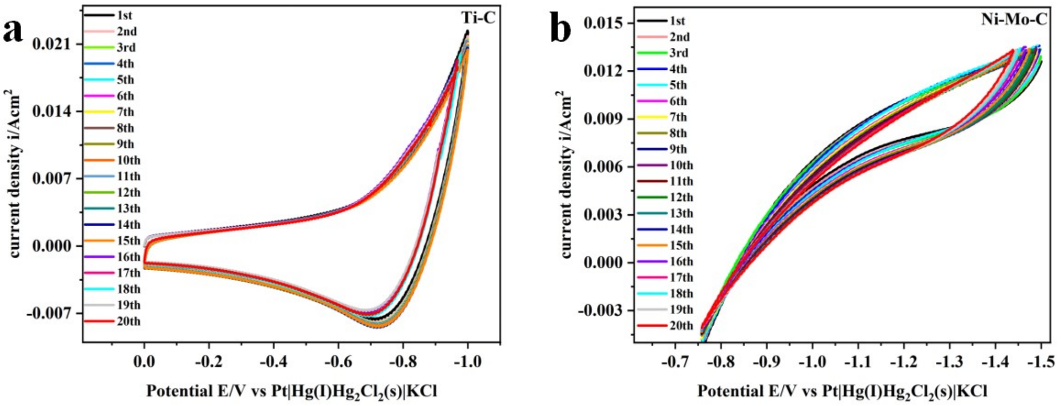

Figure S10. cyclic voltammograms of 20 replicate experiments using two homemade electrodes. (a) Cyclic voltammograms of 20 electrochemical 1,4-NADH regeneration experiments using homemade Ti-C composite electrodes for a concentration of 5 mmol/L NAD$^+$ reactant (b) Cyclic voltammograms of 20 electrochemical 1,4-NADH regeneration experiments using homemade Ni-Mo-C composite electrodes for a concentration of 5 mmol/L NAD$^+$ reactant.

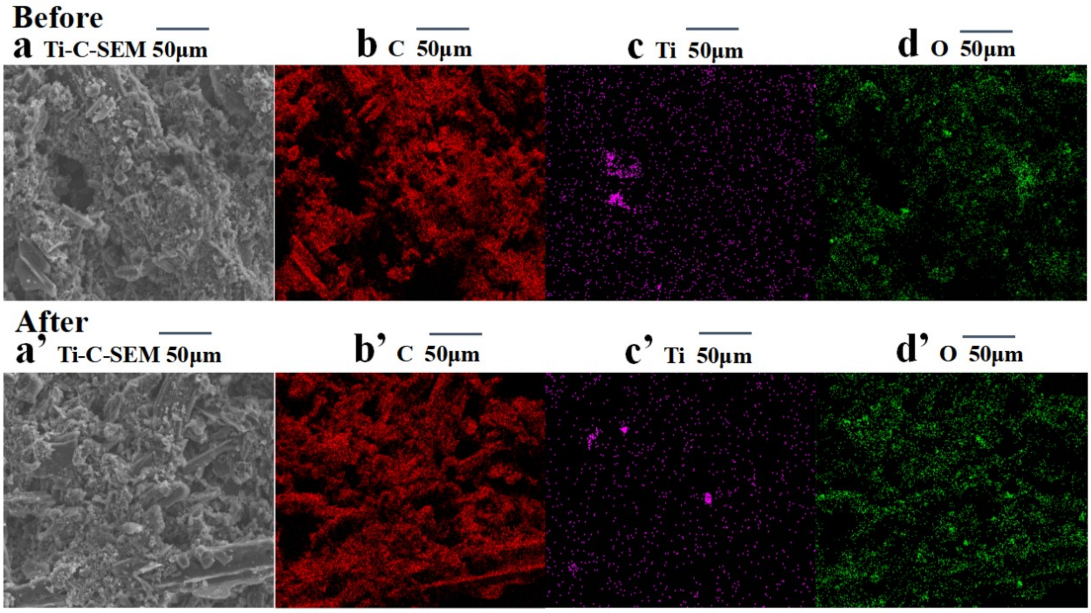

Figure S11. SEM-EDS plots of the homemade Ti-C composite electrode after 20 cycles and before the first reaction. Where a-d are the electrode surface morphology and its elemental distribution before the reaction of the homemade Ti-C composite electrode. a'-d' are the electrode surface morphology and its elemental distribution after 20 reactions of the homemade Ti-C composite electrode.

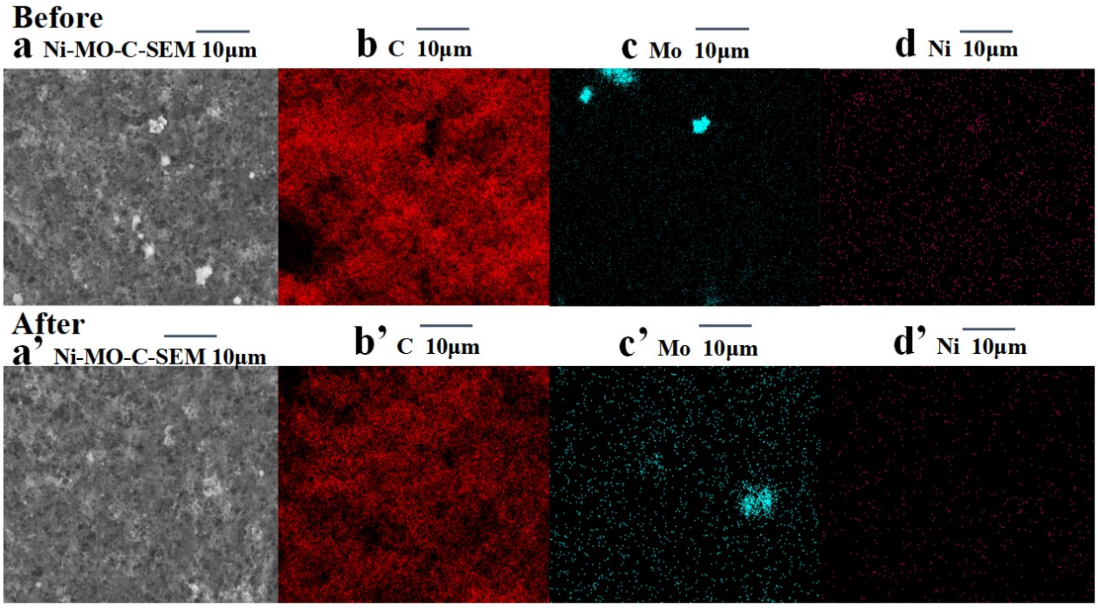

Figure S12. SEM-EDS plots of the homemade Ni-Mo-C composite electrode after 20 cycles and before the first reaction. Where a-d are the electrode surface morphology and its elemental distribution before the reaction of the homemade Ti-C composite electrode. a’-d’ are the electrode surface morphology and its elemental distribution after 20 reactions of the homemade Ti-C composite electrode.

Table S1. Conditions and maximum yields for electrochemical regeneration of 1,4-NADH by various metals and their optimized electrode materials

List	Electrode material	Optimum regeneration potential (V)	Optimum recovery time(minutes)	1,4-NADH regeneration yield %
1	Pt foil	-1.4	30	59.2
2	Pd foil	-1.4	15	93.3
3	Ni-Mo	-1.4	20	94.5
4	Ti foil	-0.8	20	95.5
5	Ni-Mo foam	-1.4	15	97.0
6	Ti foam	-0.7	15	97.6
7	Ni-Mo foam (GN)	-1.3	10	99.0
8	Ti foam (GN)	-0.7	5	99.3
9	Ni-Mo-C	-1.3	5	99.1
10	Ti-C	-0.7	5	99.3